Supporting Information

Electrocatalytic hydrogenation of furfural over copper nitride with enhanced hydrogen spillover performance

Huiming Wen[1,#], Tianchun Li[1,#], Ziyi Fan[1], Yu Jing[1,], Wenjun Zhang[1,*] and Zupeng Chen[1,*]*

[1]Jiangsu Co-Innovation Center of Efficient Processing and Utilization of Forest Resources, International Innovation Center for Forest Chemicals and Materials, College of Chemical Engineering, Nanjing Forestry University, Longpan Road 159, Nanjing 210037, China.

Email: *yujing@njfu.edu.cn; *zhangwj@njfu.edu.cn; *czp@njfu.edu.cn

[#]These authors contributed equally to this work.

Table of Contents

Supplementary Figures, Schemes and Tables

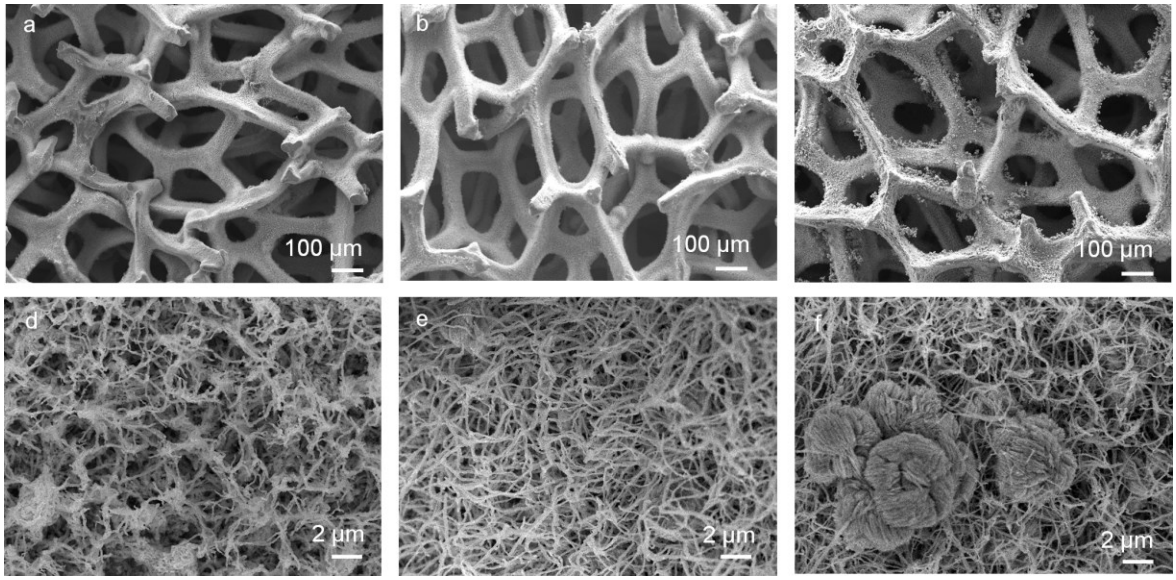

Figure S1. SEM images of (a, d) Cu_3N Nw/CF_{10}, (b, e) Cu_3N Nw/CF, and (c, f) Cu_3N Nw/CF_{30}

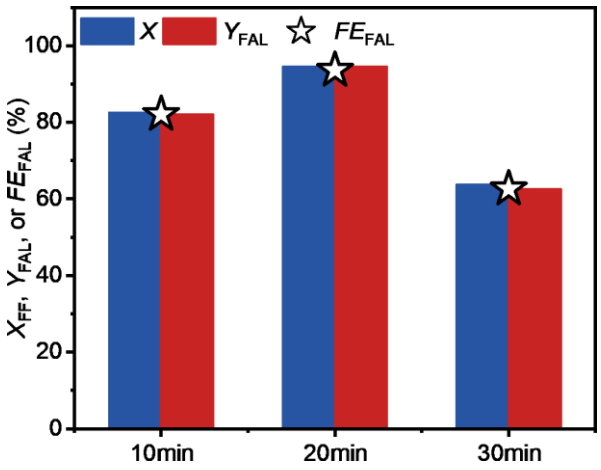

Figure S2. Performance of Cu_3N catalysts with different chemical treatment times for the catalytic conversion of FF. (electrolyte of PBS containing 20 mM FF, pH = 7, at -0.55 V *vs.* RHE, passing charges of -154 C)

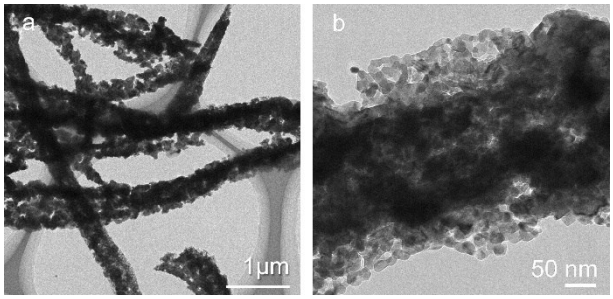

Figure S3. (a) TEM and (b) HRTEM images of Cu_3N Nw/CF.

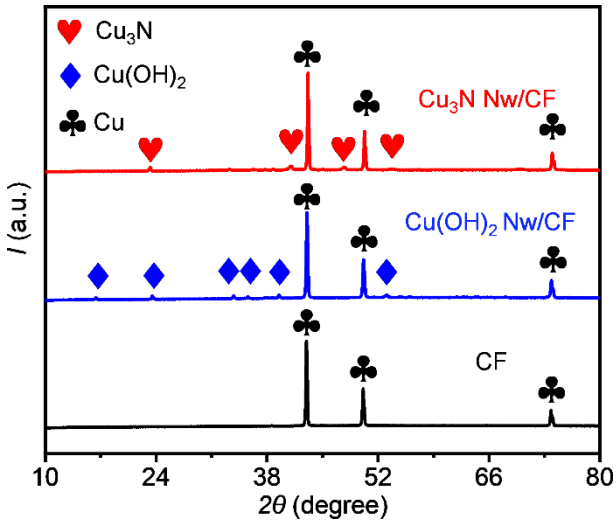

Figure S4. XRD patterns of CF, $Cu(OH)_2$ Nw/CF, and Cu_3N Nw/CF.

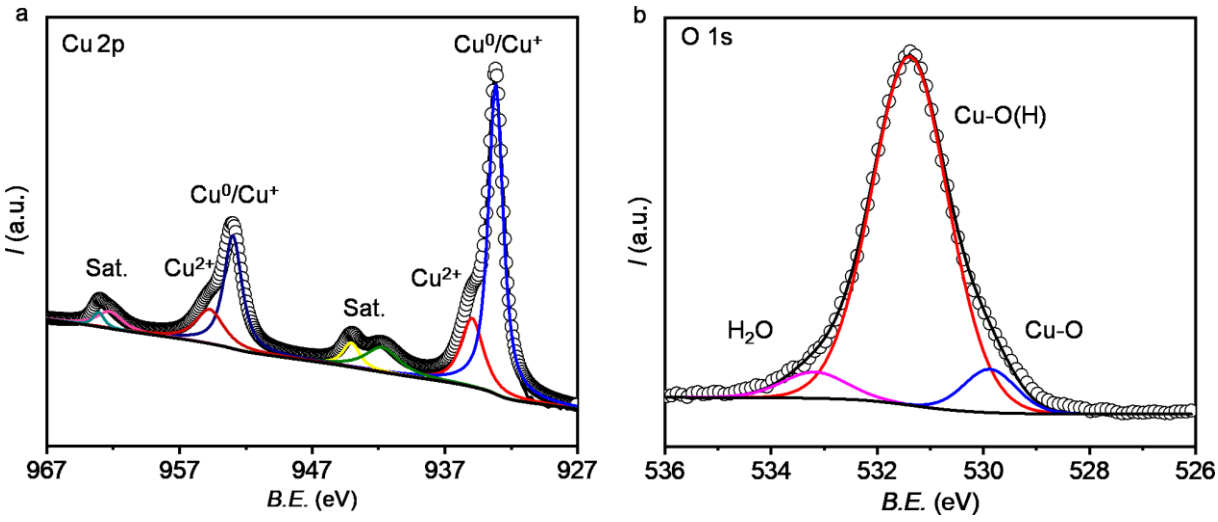

Figure S5. (a) Cu 2p and (b) O 1s XPS spectra of Cu_3N Nw/CF.

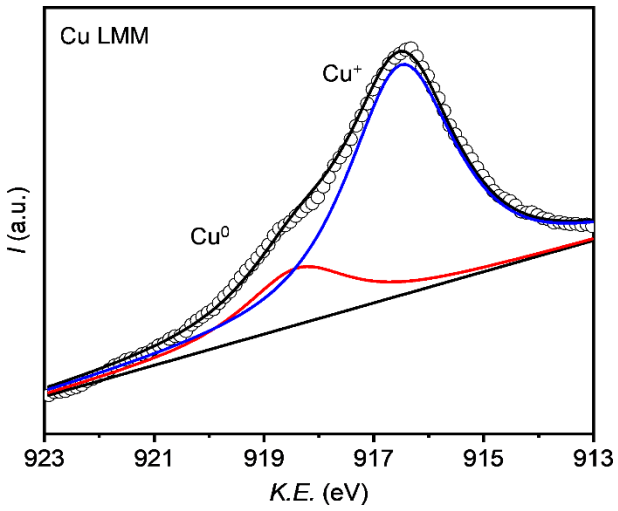

Figure S6. Cu LMM spectrum of Cu_3N Nw/CF.

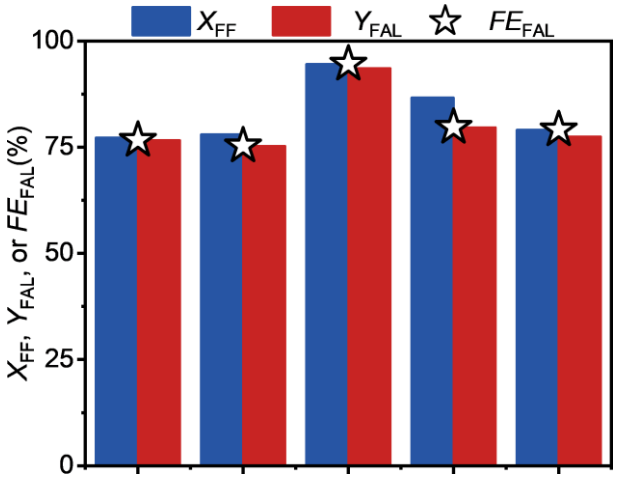

Figure S7. The dependence of the performance of ECH of FF-to-FAL upon pH of the PBS electrolyte over Cu_3N Nw/CF.

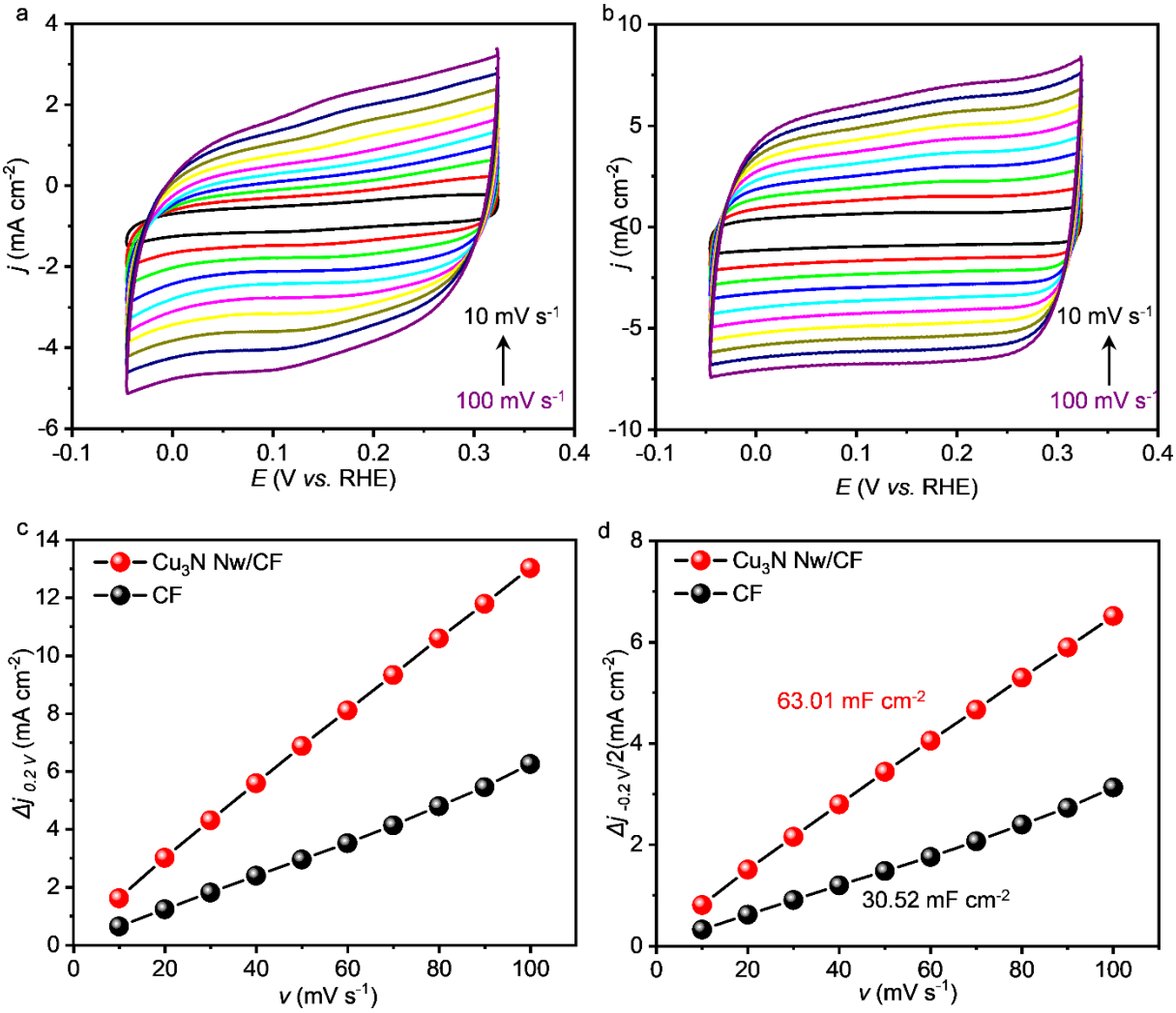

Figure S8. CV curves of (a) CF and (b) Cu_3N Nw/CF at different scan rates in 1 M KOH solution. (c) Current density difference Δj ($j_a - j_c$) at various scanning rates, and (d) double layer capacitance (C_{dl}) measured by CV.

The specific capacitance (C_s) was reported to be 0.045 mF cm^{-2}. The electrochemically active surface area of CF and Cu_3N Nw/CF was calculated by ECSA = $A*C/C_s$, where C_s = 0.045 mF cm^{-2}, A = geometric area. The results of the calculations are presented in **Table S1**.

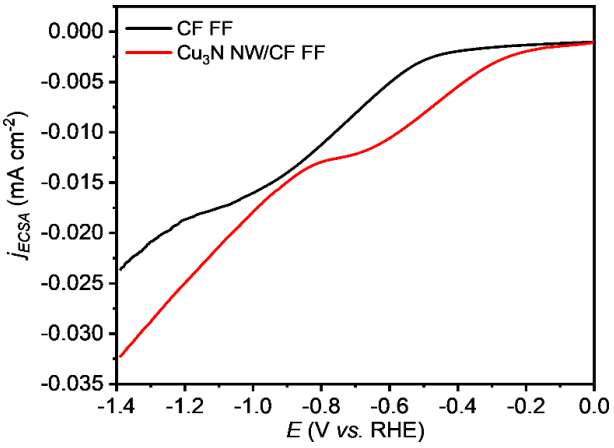

Figure S9. LSV curves of CF and Cu_3N Nw/CF corrected by ECSA in 0.1 M PBS (pH = 7) with 20 mM FF.

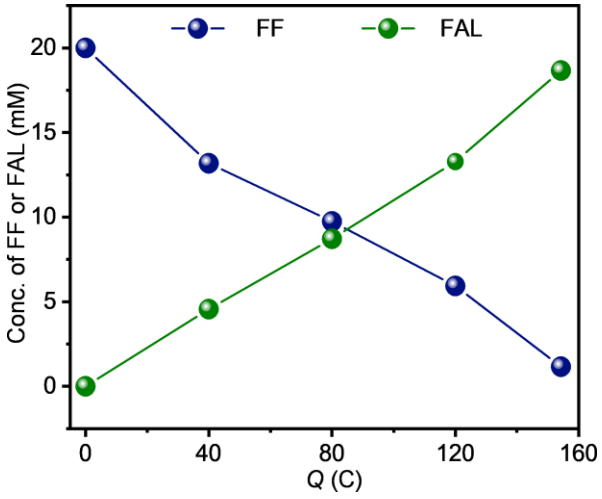

Figure S10. The corresponding concentration changes of FF and FAL with passing charges.

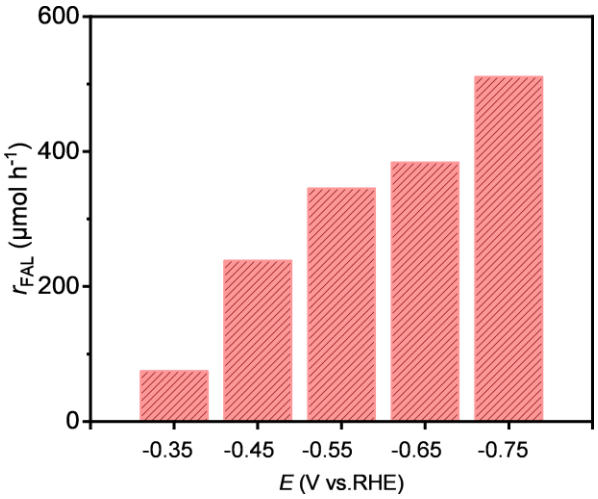

Figure S11. Generation rates of FAL over Cu_3N Nw/CF catalysts at different potentials.

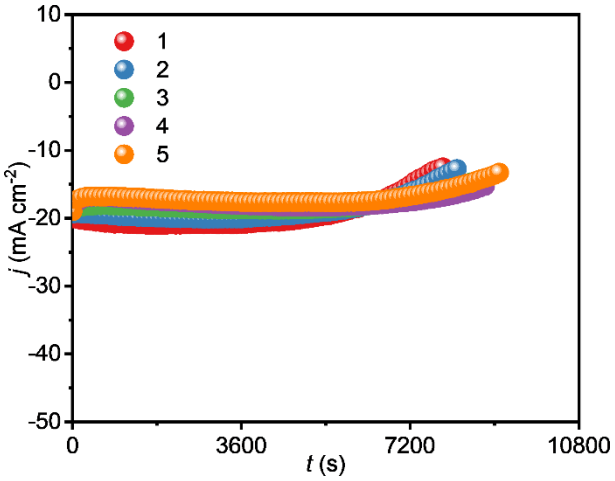

Figure S12. Chronoamperometric curves for Cu_3N Nw/CF catalyst. (electrolyte was a PBS solution containing 20 mM FF)

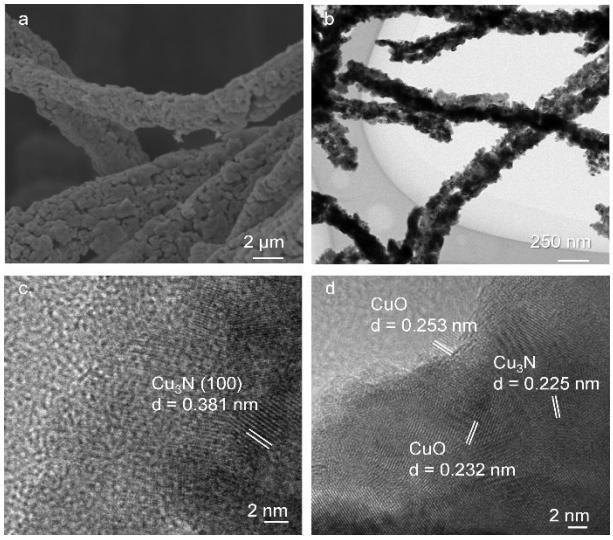

Figure S13. (a) SEM, and (b-d) (HR) TEM images of the used Cu_3N Nw/CF.

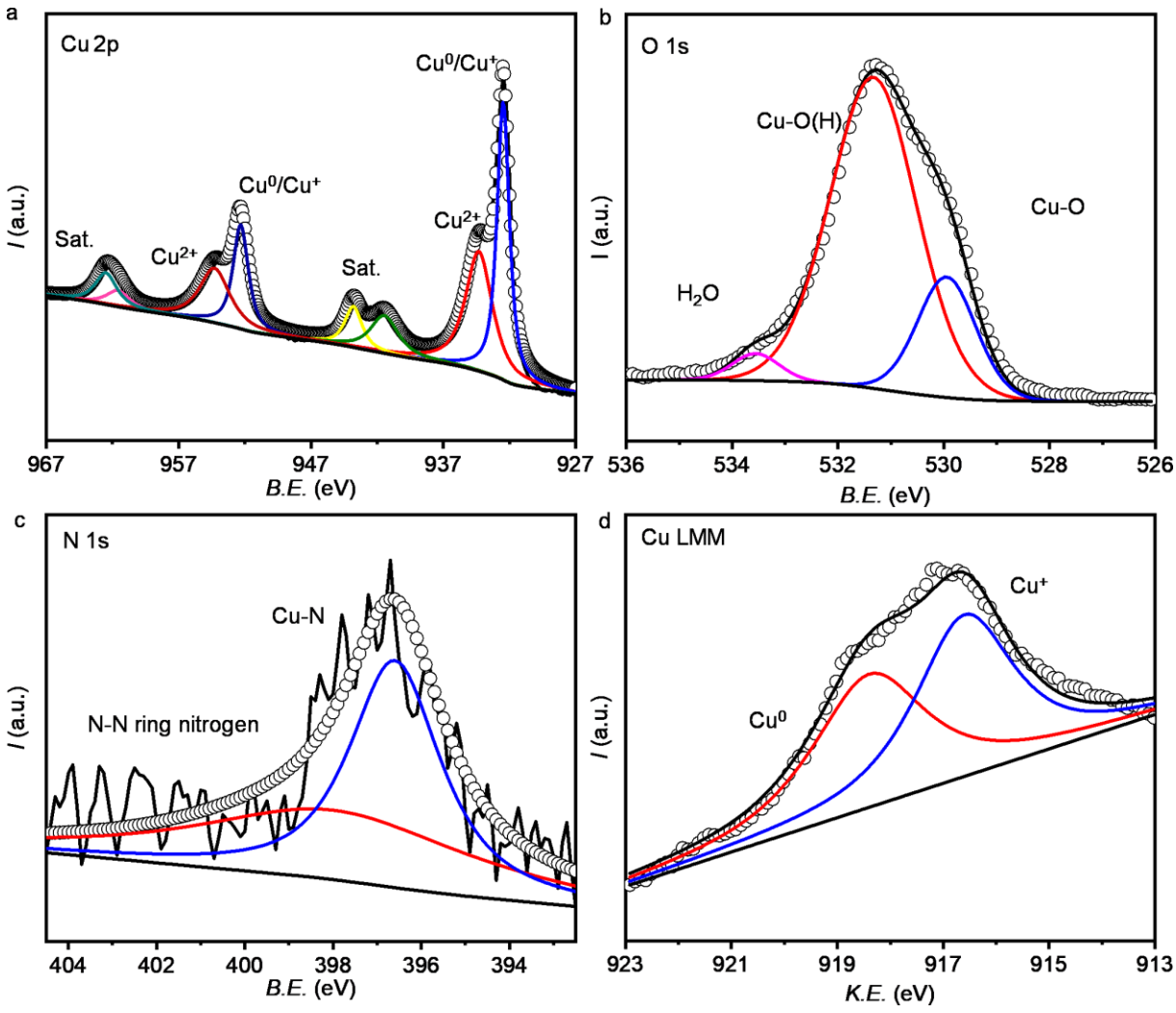

Figure S14. XPS spectra of (a) Cu $2p_{3/2}$, (b) O 1s, (c) N 1s, and (d) Cu LMM spectra of the used Cu_3N Nw/CF.

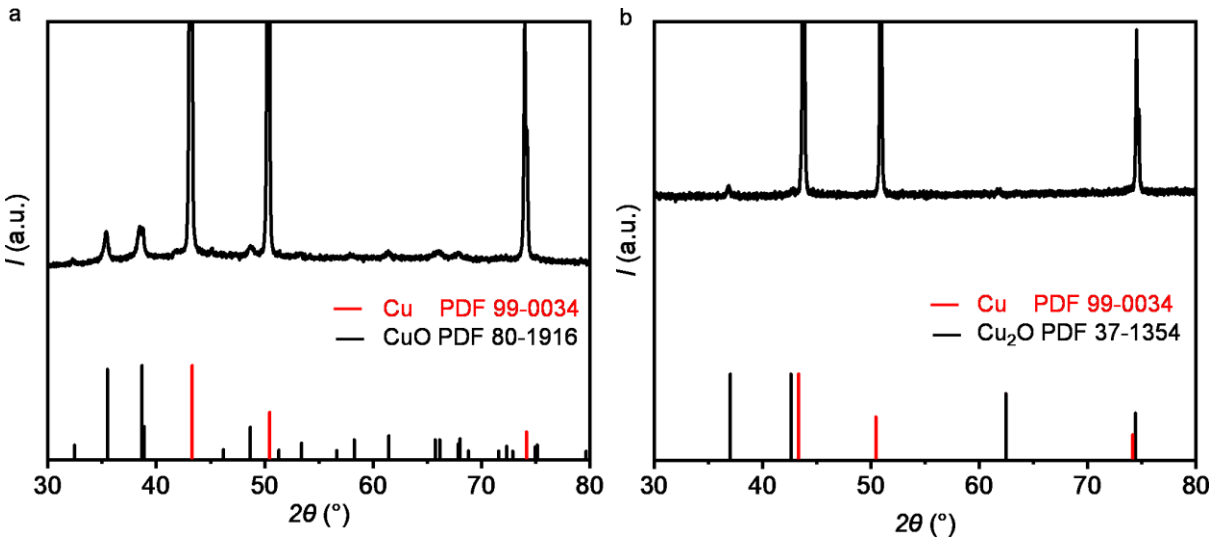

Figure S15. XRD patterns of (a) CuO Nw/CF, and (b) Cu_2O/CF.

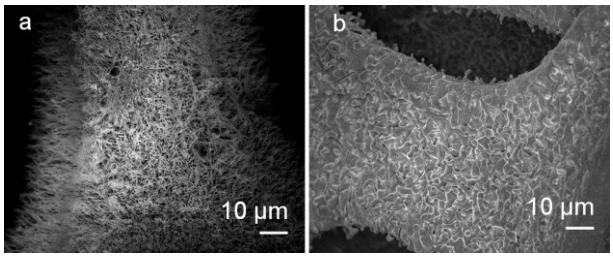

Figure S16. SEM images of (a) CuO Nw/CF, and (b) Cu_2O/CF.

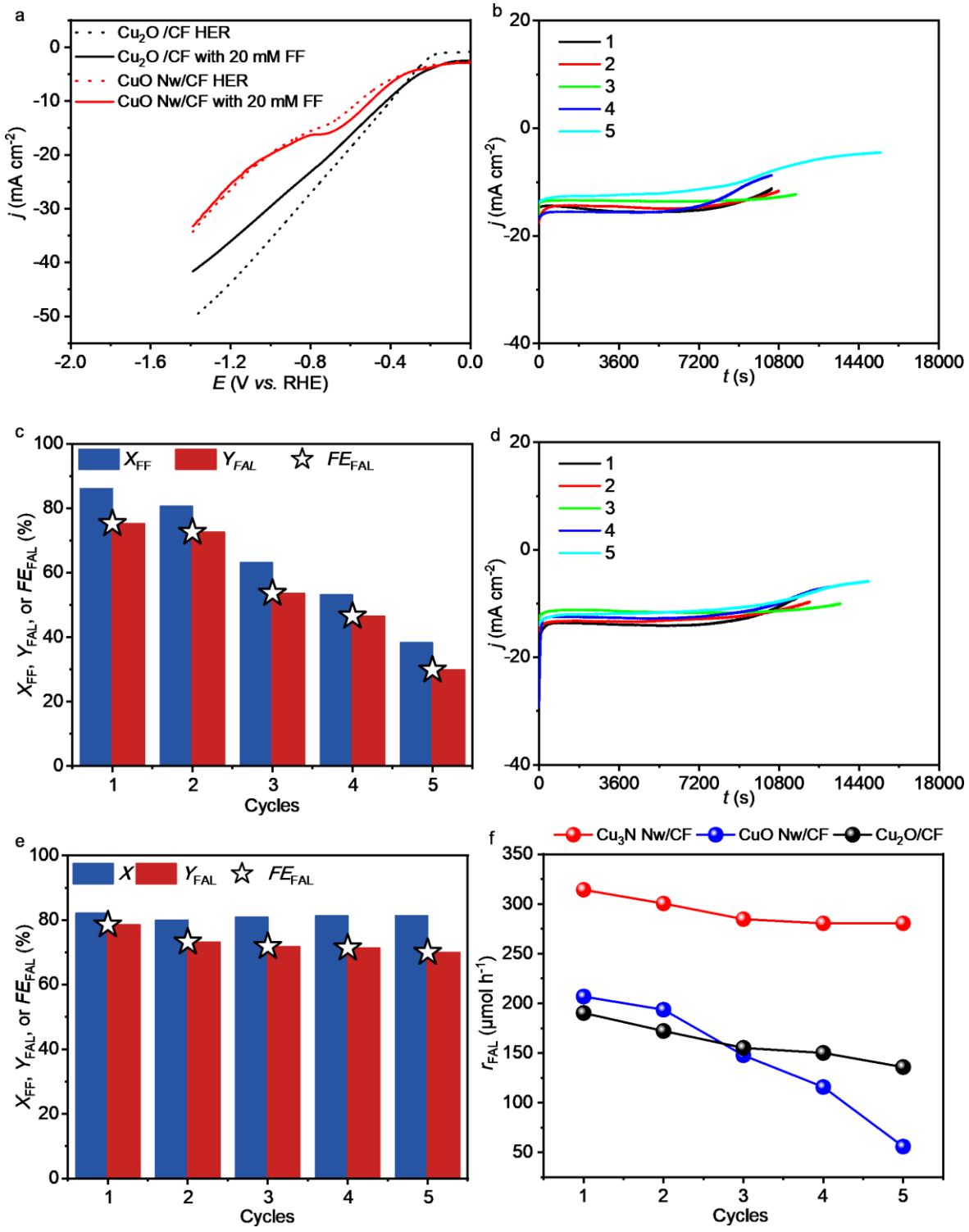

Figure S17. (a) LSV curves of CuO Nw/CF and Cu_2O/CF before and after the addition of 20 mM FF. Chronoamperometric curves over (b) CuO Nw/CF, and (d) Cu_2O/CF. ECH of FF activity over (c) CuO Nw/CF, and (e) Cu_2O/CF. (f) Generation rates of FAL over CuO Nw/CF, Cu_2O/CF and Cu_3N Nw/CF. (electrolyte of PBS containing 20 mM FF, pH = 7, at -0.55 V *vs.* RHE, passing charges of -154 C)

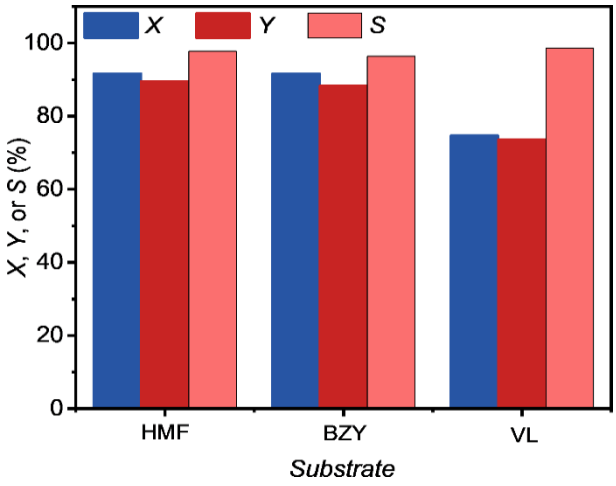

Figure S18. Hydrogenation activity of Cu_3N Nw/CF catalysts on other substrates (HMF, BZY, and VL, *X*, *Y*, *S* represent the conversion of substrate, yield and selectivity of the product, respectively). The products were the corresponding $2e^-$ reduced alcohols, the electrolyte was a PBS solution containing 20 mM aldehyde, passing 154 C charge.

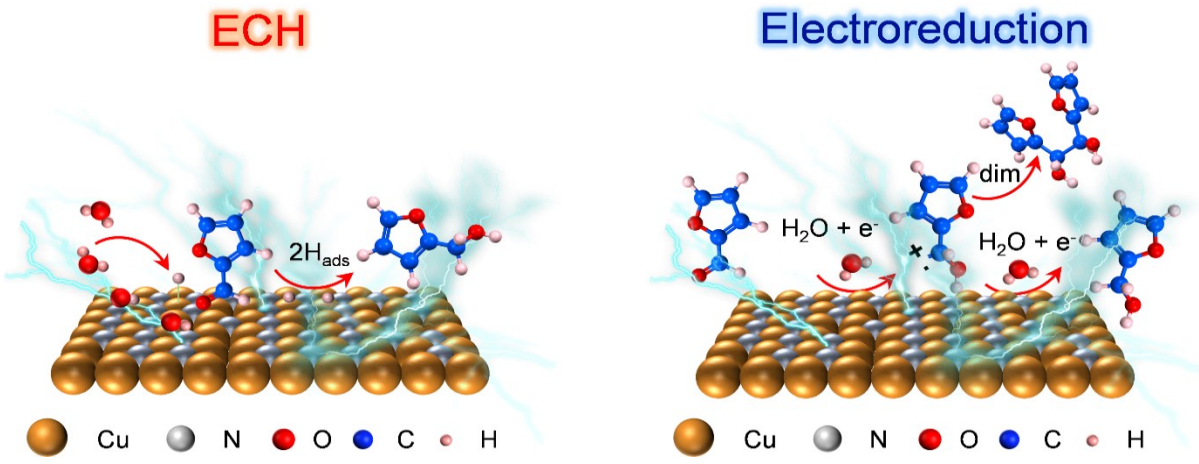

Figure S19. The schematic of ECH and electroreduction processes over Cu_3N Nw/CF catalyst.

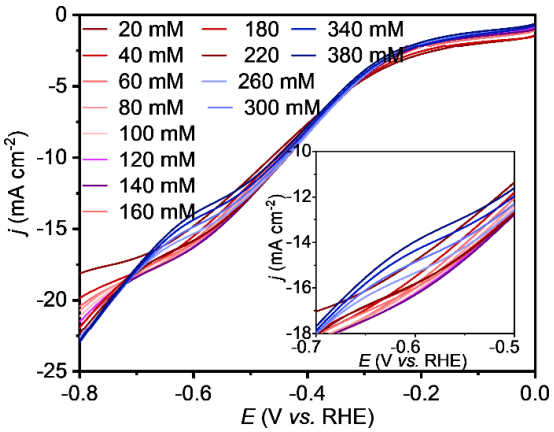

Figure S20. LSV curves for different concentrations of FF in 0.1M PBS over Cu_3N Nw/CF.

Our experiments have demonstrated that the adsorption competition between H_3O^+ and furfural over Cu_3N Nw/CF catalysts involves. According to the work of Lopez-Ruiz,[1] the rate expression for the Langmuir-Hinshelwood (L-H) competitive adsorption of furfural and H_3O^+ is as follows:

$$r_{LH}=\frac{k_T\cdot K_{FF}\cdot[FF]\cdot(K_H\cdot a_{H_3O^+})^2}{(1+K_{FF}\cdot[FF]+K_H\cdot a_{H_3O^+})^3} \quad (9)$$

Where k_T is the kinetic constant of the hydrogenation step, K_{FF} is the adsorption equilibrium constant of the furfural, [FF] is the concentration of furfural, K_H is the adsorption equilibrium constant of H_3O^+, and $a_{H_3O^+}$ is the activity of H_3O^+.

At low surface coverage (or low concentration) of furfural, $K_{FF}\cdot[FF] << 1$, the formula is simplified as below:

$$r_{LH}=\frac{k_T\cdot K_{FF}\cdot[FF]\cdot(K_H\cdot a_{H_3O^+})^2}{(1+K_H\cdot a_{H_3O^+})^3} \quad (10)$$

positive order on furfural concentration.

At high surface coverage (or high concentration) of furfural, $K_{FF}\cdot[FF] >> 1$, the formula is simplified as below:

$$r_{LH}=\frac{k_T\cdot(K_H\cdot a_{H_3O^+})^2}{(K_{FF}\cdot[FF])^2} \quad (11)$$

negative order on furfural concentration.

For the Eley-Rideal competitive adsorption of furfural and H_3O^+ can expression for the as follow:

$$r_{ER}=\frac{k_T\cdot K_{FF}\cdot[FF]\cdot K_H\cdot a_{H_3O^+}{}^2}{1+K_{FF}\cdot[FF]+K_H\cdot a_{H_3O^+}} \quad (12)$$

At low surface coverage (or low concentration) of furfural, $K_{FF}\cdot[FF] << 1$, the formula is simplified as:

$$r_{ER}=\frac{k_T\cdot K_{FF}\cdot[FF]\cdot K_H\cdot a_{H_3O^+}{}^2}{1+K_H\cdot a_{H_3O^+}} \quad (13)$$

positive order on furfural concentration.

At high surface coverage (or high concentration) of furfural, $K_{FF}\cdot[FF] >> 1$, the formula is simplified as:

$$r_{ER}=k_T\cdot a_{H_3O^+} \quad (14)$$

zero order on furfural concentration.

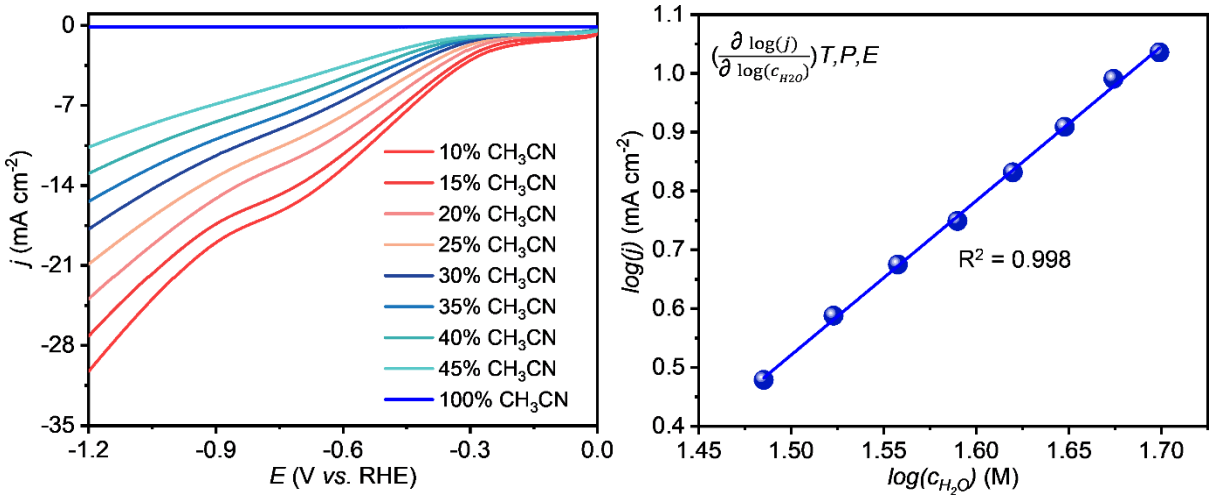

Figure S21. (a) LSV curves of different acetonitrile contents over Cu_3N Nw/CF in 0.1M PBS (pH = 7) containing 20 mM FF. (b) Correlation curve between water content and current density.

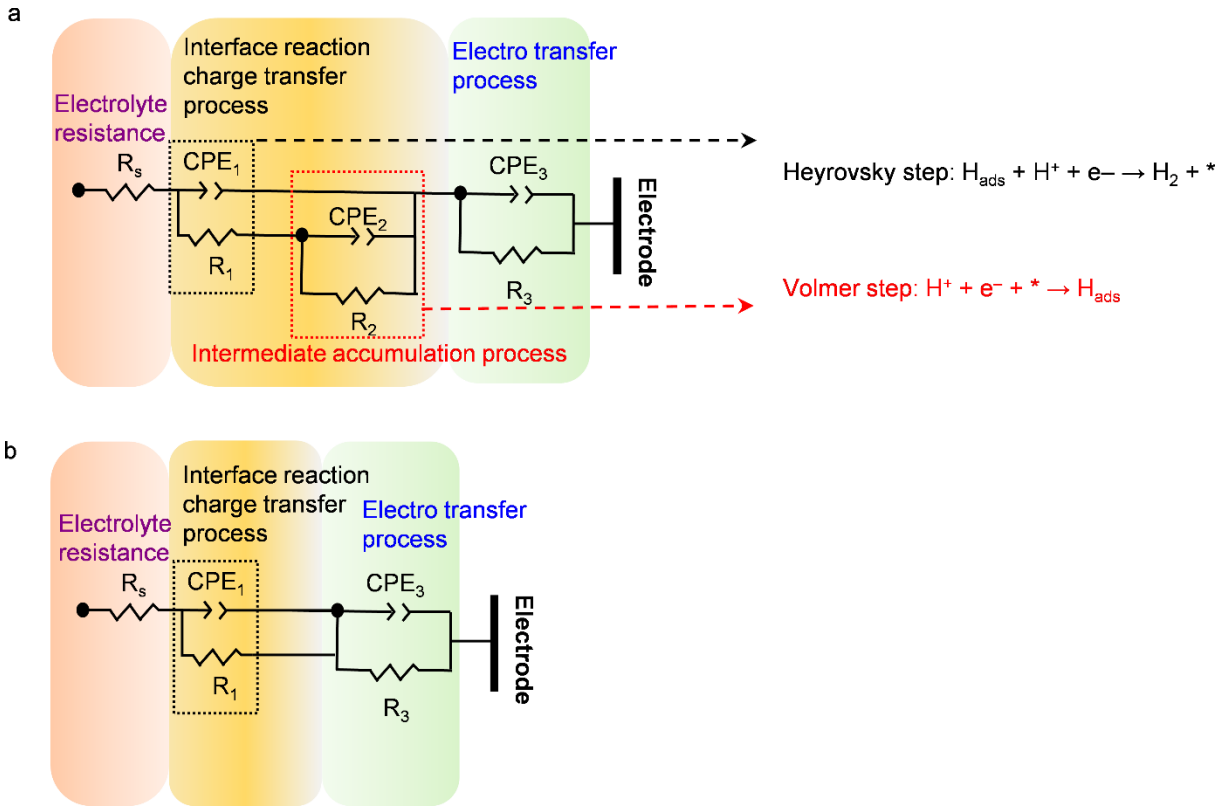

Figure S22. (a) Equivalent circuit diagram for CF and Cu_3N Nw/CF. (b) Simplified equivalent circuit for CF and Cu_3N Nw/CF at higher potential.

The equivalent circuit of CF and Cu_3N Nw/CF consists of four parts: (1) electron transfer from the catalysts to the reaction interface, (2) the intermediate accumulation process at the reaction interface, (3) interfacial reaction charge transfer process and (4) electrolyte resistance. Since the low-frequency relaxation rapidly decreases to high frequencies at high potentials, the intermediate accumulation process can be neglected, and the equivalent circuit diagram is correspondingly simplified as **Figure S22b**.

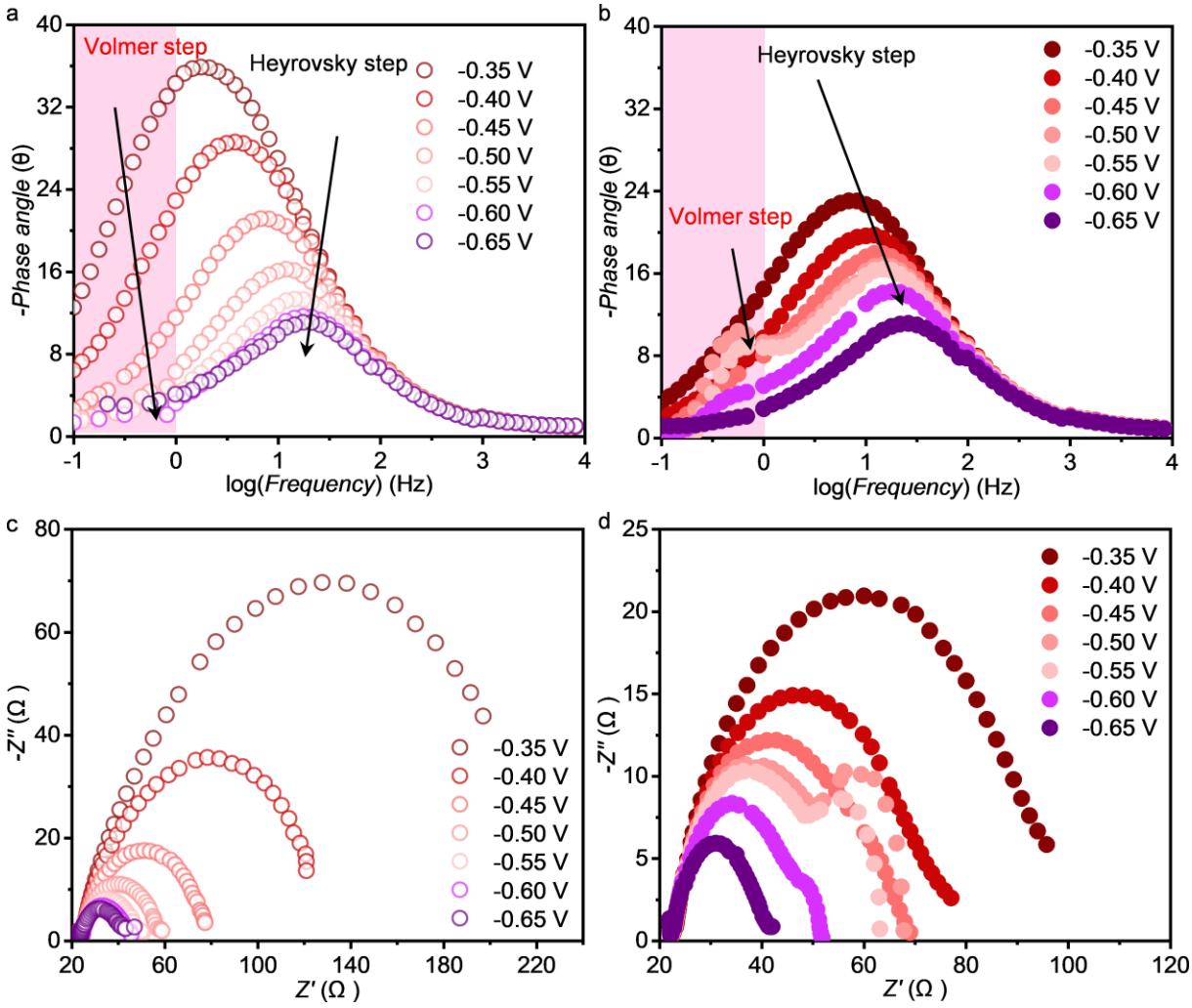

Figure S23. Bode plots for CF at different potentials in PBS (pH = 7) (a) without and (b) with the addition of 20 mM FF. Nyquist plots for CF at different potentials in PBS (pH = 7) (c) without and (d) with the addition of 20 mM FF.

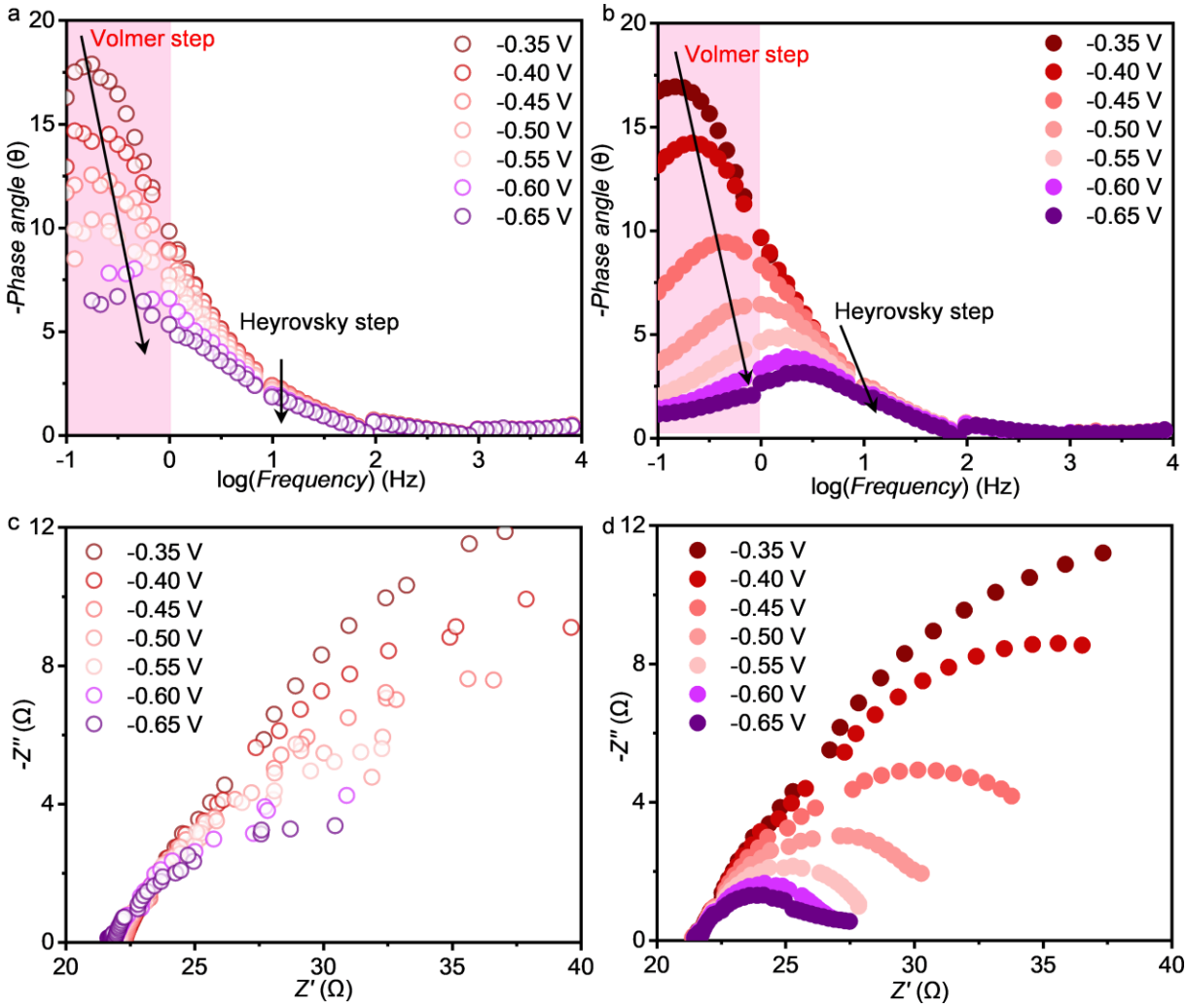

Figure S24. Bode plots for Cu_3N Nw/CF at different potentials in PBS (pH = 7) (a) without and (b) with the addition of 20 mM FF. Nyquist plots for Cu_3N Nw/CF at different potentials in PBS (pH = 7) (c) without and (d) with the addition of 20 mM FF.

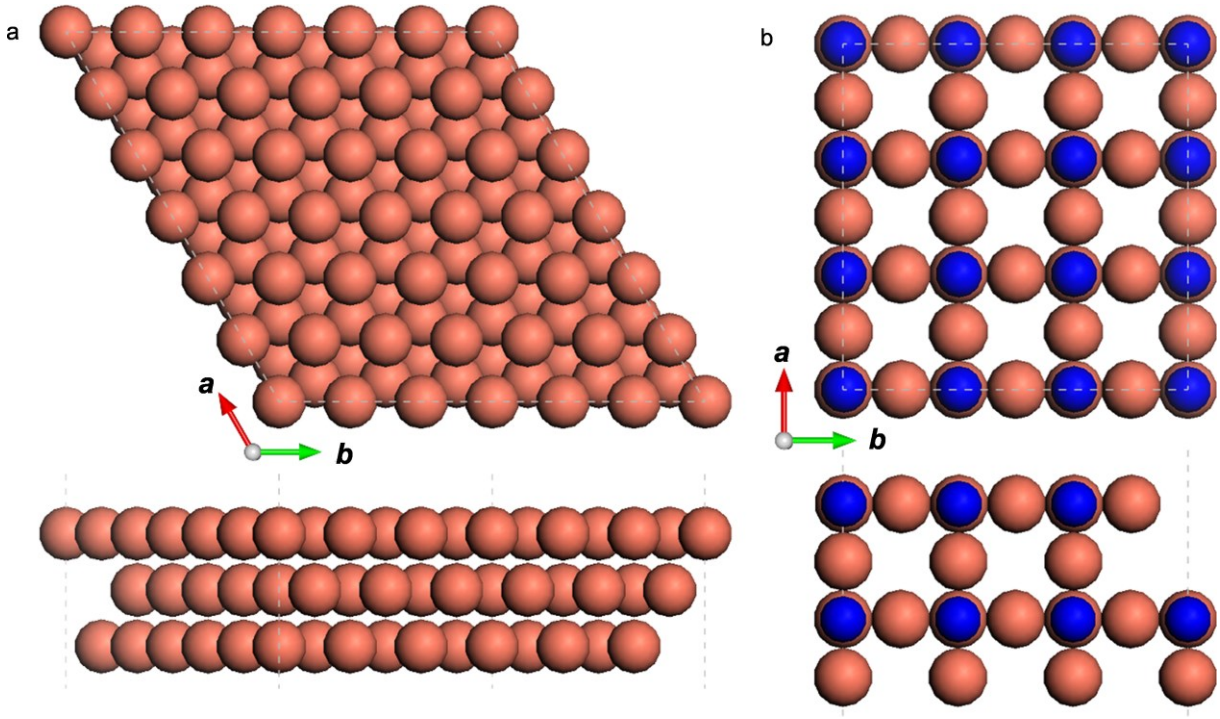

Figure S25. Structure schematics of (a) Cu(111) and (b) Cu_3N(100) surfaces, in which the lattice of the 3×3×1 supercell is indicated by the gray dashed line. The orange and blue atoms represent Cu and N atoms, respectively.

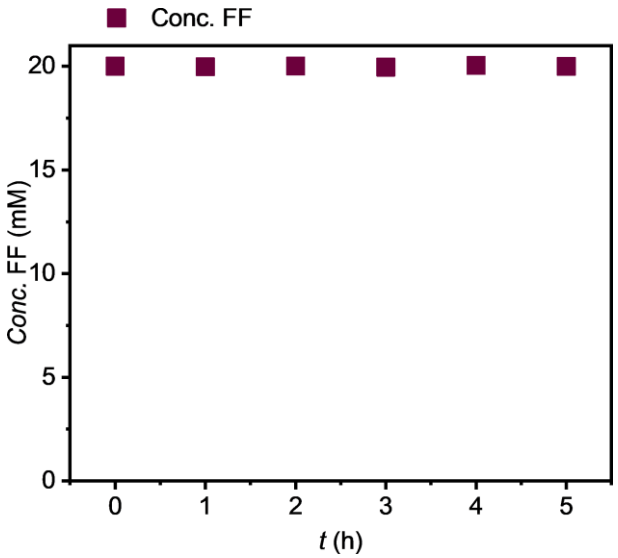

Figure S26. Stability of FF in 0.1M PBS (pH = 7)

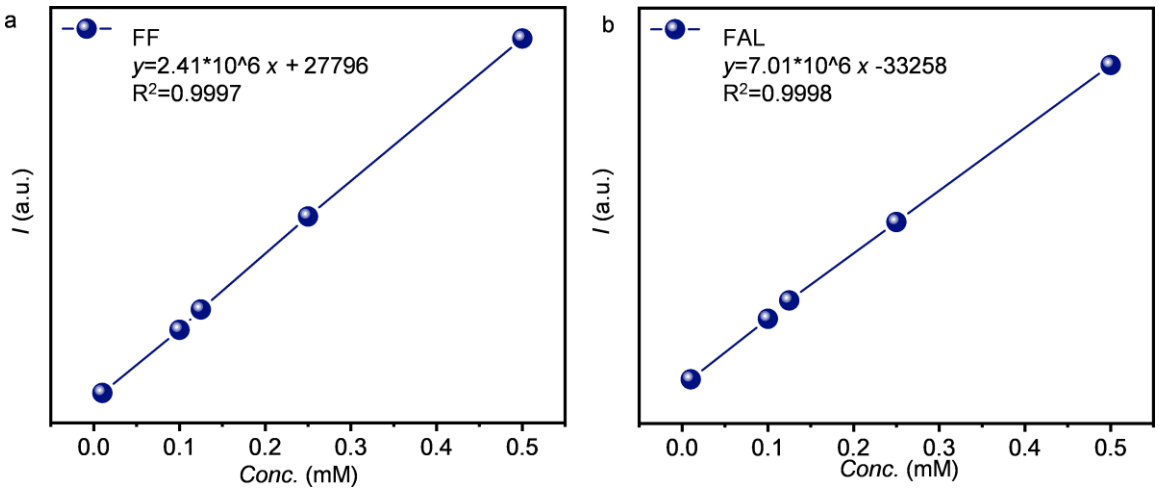

Figure S27. Calibration curves of HPLC for (a) FF and (b) FAL.

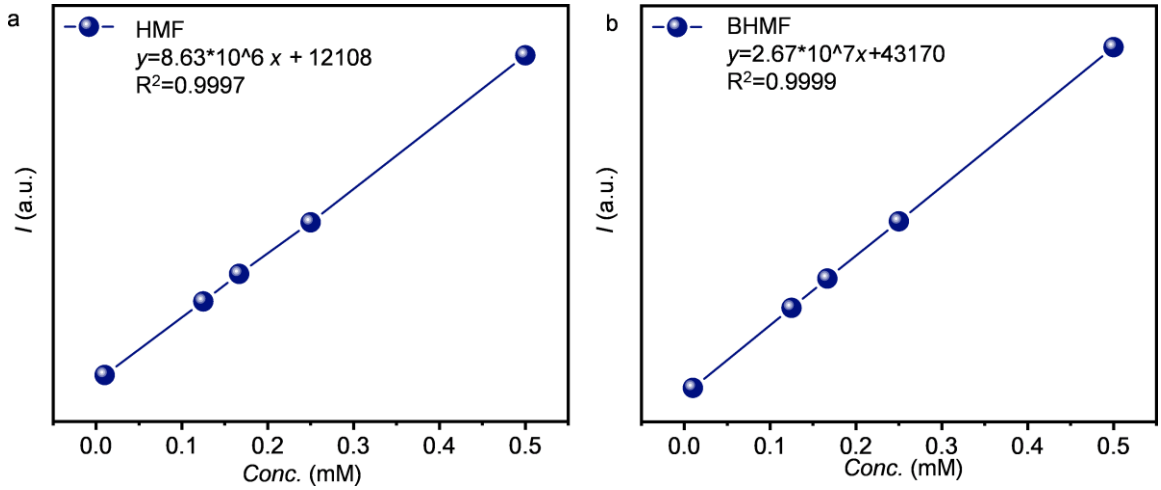

Figure S28. Calibration curves of HPLC for (a) HMF and (b) BHMF.

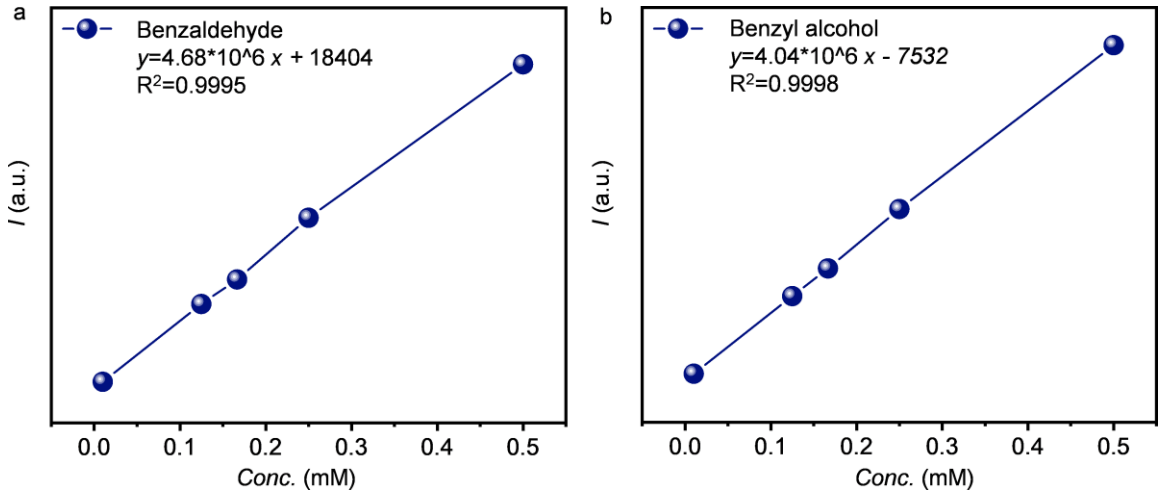

Figure S29. Calibration curves of HPLC for (a) Benzaldehyde and (b) Benzyl alcohol.

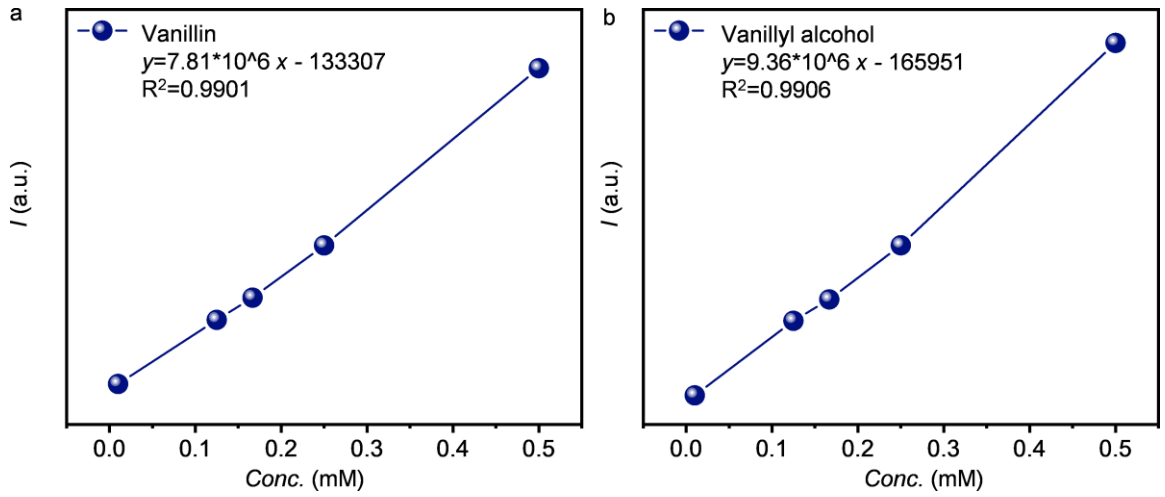

Figure S30. Calibration curves of HPLC for (a) Vanillin and (b) Vanillyl alcohol.

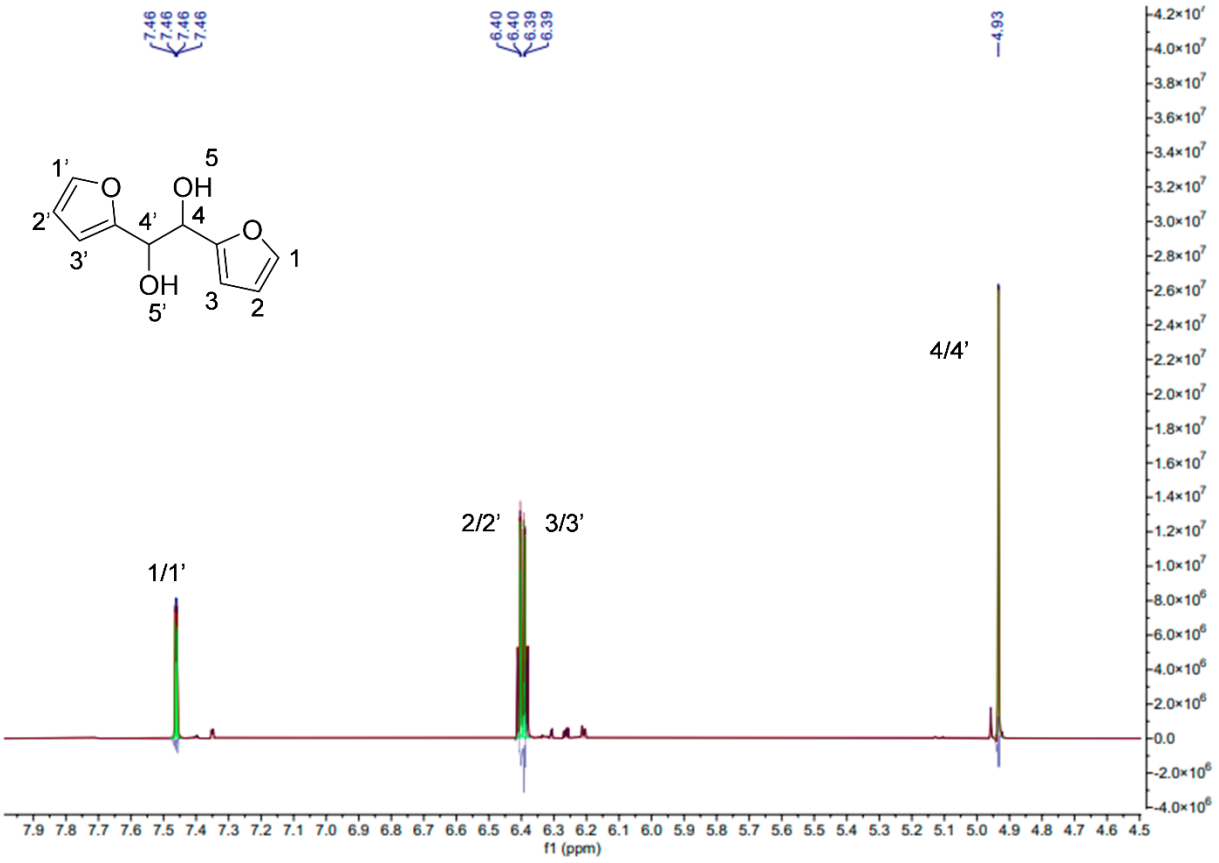

Figure S31. [1]H-NMR spectra of the home-made HFN.

[1]H NMR (400 MHz, H_2O+D_2O) δ 7.46, 7.46, 7.46, 7.46, 6.40, 6.40, 6.39, 6.39, 4.93.

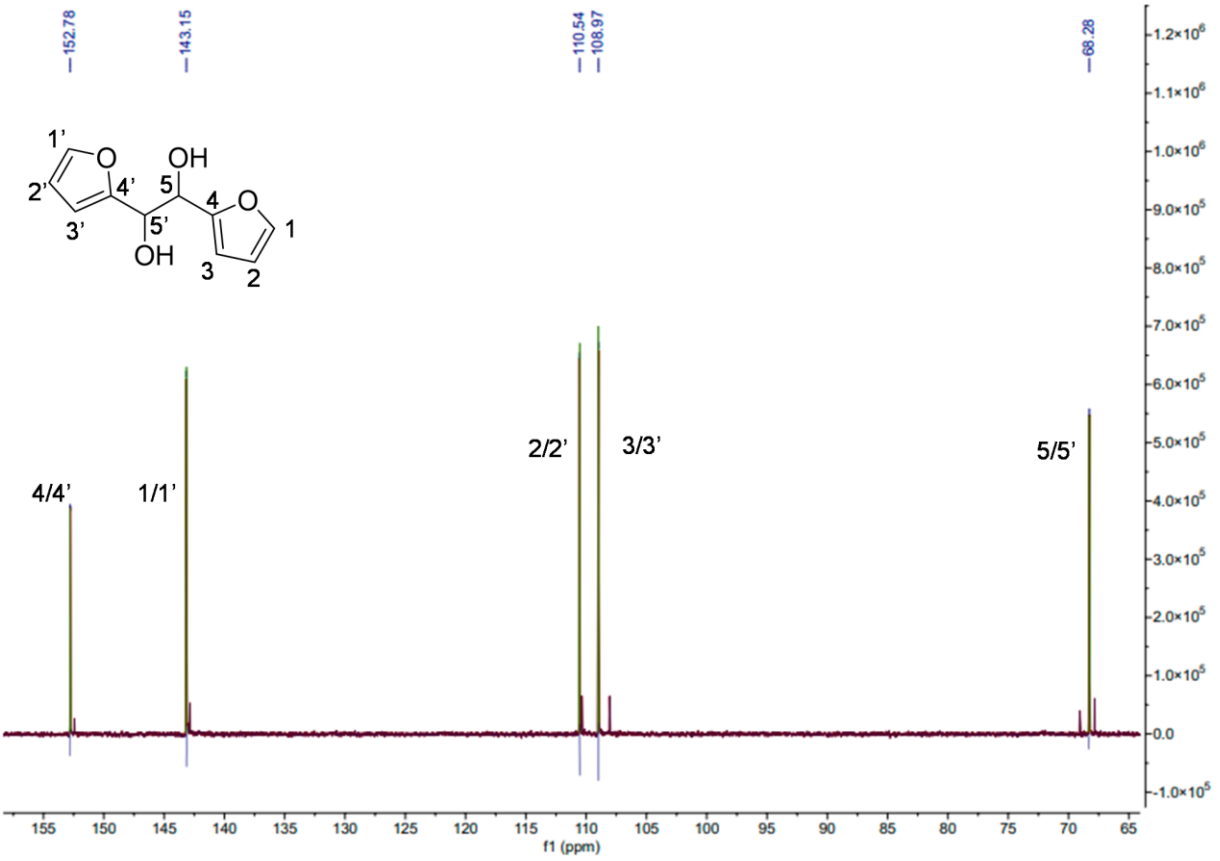

Figure S32. ^{13}C-NMR spectra of the home-made HFN.

^{13}C NMR (101 MHz, H_2O+D_2O) δ 152.78, 143.15, 110.54, 108.97, 68.28.

Table S1. C_{dl} and ECSA of CF and Cu_3N Nw/CF.

Catalysts	C_{dl} (mF cm^{-2})	ECSA (cm^2)
CF	30.52	678.2
Cu_3N Nw/CF	63.01	1400.2

Table S2. Optimum fit parameters for the electrochemical impedance spectra of CF in 0.1 M PBS.

Electrolyte	Potential (V vs. RHE)	Rs (Ω cm^2)	CPE_1-T	CPE_2-P	R_1 (Ω cm^2)	CPE_1-T	CPE_2-P	R_2 (Ω cm^2)	CPE_1-T	CPE_2-P	R_3 (Ω cm^2)
0.1M PBS	-0.35	22.92	0.009656	0.5979	30.57	0.008776	1.25	52.95	0.002180	0.8377	135.4
	-0.40	22.1	0.02649	0.1524	4.63	0.008979	1.129	42.72	0.001850	0.7828	81.69
	-0.45	22.56	0.03062	0.1071	7.141	0.097329	4.001	6.29	0.001715	0.7958	31.28
	-0.50	23.9	0.003630	0.7192	32.93	0.008338	1.315	0.14	0.004177	0.7964	21.38
	-0.55	22.53	0.1957	0.1291	1.0818E7	0.008256	1.245	0.26	0.001758	0.8112	21.45
	-0.60	22.21	0.1616	0.1347	3.2906E6				0.001789	0.8205	16.97
	-0.65	22.14	0.13808	0.1702	2.2279E7				0.001782	0.8362	14.32

Table S3. Optimum fit parameters for the electrochemical impedance spectra of CF in 0.1 M PBS with 20 mM FF.

Electrolyte	Potential (V vs. RHE)	Rs (Ω cm^2)	CPE_1-T	CPE_2-P	R_1 (Ω cm^2)	CPE_1-T	CPE_2-P	R_2 (Ω cm^2)	CPE_1-T	CPE_2-P	R_3 (Ω cm^2)
0.1 M PBS +20 mM FF	-0.35	21.48	0.001726	0.7431	62.09	0.01802	0.8451	10.56	0.04525	0.75539	42.26
	-0.40	22.08	0.09093	0.3142	38.76	0.02965	0.005439	0.57	0.001851	0.7642	12.19
	-0.45	22.19	0.007814	0.5614	34.06	0.06468	0.04843	0.37	0.001641	0.9107	14.85
	-0.50	22.35	0.001533	0.7619	32.03	0.04948	0.06533	9.794	0.07442	1.637	3.088
	-0.55	22.37	0.001364	0.7855	28.8	0.05345	0.04635	6.586	0.02121	1.304	2.582
	-0.60	22.2	0.001700	0.7455	25.88				0.07236	1.322	2.672
	-0.65	22.12	0.001812	0.7355	18.4				0.3466	1.005	1.16

Table S4. Optimum fit parameters for the electrochemical impedance spectra of Cu_3N Nw/CF in 0.1 M PBS.

Electrolyte	Potential (V vs. RHE)	Rs (Ω cm^2)	CPE_1-T	CPE_2-P	R_1 (Ω cm^2)	CPE_1-T	CPE_2-P	R_2 (Ω cm^2)	CPE_1-T	CPE_2-P	R_3 (Ω cm^2)
0.1 M PBS	-0.35	22.23	0.03901	0.7210	3.5425	0.04335	0.7661	36.12	0.04498	0.8508	52.85
	-0.40	22.17	0.04099	0.6935	3.2023	0.04167	0.80484	20.68	0.04374	0.7541	28.12
	-0.45	22.12	0.04420	0.6812	2.6532	0.04008	0.7640	10.79	0.04422	0.5318	26.24
	-0.50	21.96	0.05076	0.6502	2.2623	0.04176	0.8321	5.26	0.04882	0.7954	17.67
	-0.55	21.84	0.04795	0.6901	1.9665				0.04441	0.8442	13.04
	-0.60	21.78	0.05582	0.0558	1.6945				0.05813	0.7303	7.84
	-0.65	21.75	0.04566	0.7104	1.3934				0.05103	0.8308	6.79

Table S5. Optimum fit parameters for the electrochemical impedance spectra of Cu_3N Nw/CF in 0.1 M PBS. with 20 mM FF.

Electrolyte	Potential (V vs. RHE)	Rs (Ω cm^2)	CPE_1-T	CPE_2-P	R_1 (Ω cm^2)	CPE_1-T	CPE_2-P	R_2 (Ω cm^2)	CPE_1-T	CPE_2-P	R_3 (Ω cm^2)
0.1 M PBS +20 mM FF	-0.35	21.48	0.0006120	3.769	2.95	0.09101	0.04724	29.96	0.05444	0.6524	40.70
	-0.40	21.51	0.0003450	3.456	2.55	2.006	3.413	15.67	0.043308	0.6938	28.01
	-0.45	21.99	0.0003433	3.917	2.03	0.06785	2.323	8.45	0.05638	0.6435	27.24
	-0.50	21.44	0.1719	0.4822	1.67	0.03576	3.950	1.556	0.03445	0.8321	5.539
	-0.55	21.46	0.1889	0.5009	1.56				0.03162	0.8161	4.358
	-0.60	21.45	0.03802	0.6931	1.18				0.1192	1.332	4.658
	-0.65	21.56	0.03072	0.76075	0.56				0.06256	0.8053	3.824

Reference

(1) Lopez-Ruiz, J. A.; Sanyal, U.; Egbert, J.; Gutiérrez, O. Y.; Holladay, J., *ACS Sustain. Chem. Eng.* **2018,** *6* (12), 16073-16085.